

# Nanostructural Transformation and Formation of Heterojunctions from Si Nanowires

Tai Lun Wong, Chun Cheng, Wei Li, Kwok Kwong Fung, and Ning Wang\*

Department of Physics and The William Mong Institute of Nano Science and Technology, the Hong Kong University of Science and Technology, Hong Kong, China

Because of the importance of Si-based materials to the electronic industry, considerable effort has been devoted to studying Si and metal silicide nanowire structures.<sup>1</sup> Nickel silicides show low electrical resistivity and excellent thermal stability without the electron migration effect at high temperatures. They are promising candidates as the electrical contacts for Si nanowire devices because of their good compatibility with Si and small lattice mismatch at the interface. The conventional methods for fabricating Ni silicide nanowires are based on the phase transformation through annealing treatment of Ni-coated Si nanowires at temperatures higher than 550 °C in vacuum.<sup>1</sup> An excess of Ni coating is normally needed and has to be removed by chemical etching after reaction. The Ni silicide nanowires obtained by annealing treatment are usually polycrystalline. Ni silicide nanowires can be directly grown on the Ni thin films (10–100 nm thick) deposited on SiO<sub>2</sub> substrates using silane as the vapor-phase Si source.<sup>2–4</sup> The growth temperature is low (about 370 °C); however, the as-grown Ni silicide nanowires are polycrystalline and contain different phases.

Lu *et al.*<sup>5,6</sup> demonstrated a novel method of point contact reaction to transform Si nanowires into single crystalline Ni silicide structures in an electron microscope. The Ni atoms could diffuse and interact with the Si nanowire to form a NiSi structure. The interface between the Si nanowire and the newly formed NiSi wire was atomic flat and epitaxial without any misfit dislocations. Beside NiSi/Si junctions, NiSi/Si/NiSi heterostructures were also synthesized using two Ni nanowires to touch one Si nanowire.<sup>6</sup> Ni displayed interesting behaviors when reacting with Si nanowires. For example, for the

**ABSTRACT** Si nanowires coated with Ni showed interesting structural transformation behaviors as observed by *in situ* transmission electron microscopy. Owing to the presence of the native oxide on Si nanowire surfaces, the Ni thin shells initially segregated into nanosized droplets on the oxide surfaces. The native oxide shells protected the Si cores from reacting with Ni at temperatures below 1350 °C. Ni started the reaction with Si nanowires preferentially at the defects or bending regions of the nanowires. Because the reaction temperature was sufficiently high, the structural transformation was extremely fast and completed within 0.1 s. The resulting nanowires were single crystalline NiSi<sub>2</sub>, the most desirable Ni silicide structure for potential applications. Nanowire junctions of NiSi<sub>2</sub>/Si and nanowire–nanotube junctions of NiSi<sub>2</sub>/SiC have been obtained upon further annealing.

**KEYWORDS:** silicon nanowire · metal silicides · structural transformation · *in situ* study · heterojunctions

point contact reaction of Ni and Si nanowires, the sites of the initial reaction or initially formed NiSi grains usually occurred at the ends of the Si nanowire rather than the contact points of the two nanowires. Moreover, because of the presence of the oxide shells on Si nanowires, the diffusion and reaction of Ni atoms through the oxide shells become complicated, and the resulted silicide nanowires included NiSi, Ni<sub>2</sub>Si, Ni<sub>31</sub>Si<sub>12</sub>, etc.<sup>7</sup>

It has been known that NiSi<sub>2</sub> nanowires are more desirable than other Ni silicide nanowires for potential applications because this crystal structure is stable at high temperature conditions and shows lower resistivity. In addition, NiSi<sub>2</sub> has the smallest lattice mismatch with cubic Si structure compared to other Ni silicides,<sup>8</sup> indicating that the interface stress in the nanowire heterostructure of NiSi<sub>2</sub>/Si should be very low. In this paper, we report *in situ* observation of the formation of single crystalline NiSi<sub>2</sub> silicide nanowires. We have found that the native oxide shells on Si nanowires greatly affected the reaction between Ni and Si. The reaction started preferentially at bending regions of the nanowires and completed

\*Address correspondence to phwang@ust.hk.

Received for review March 8, 2010 and accepted September 07, 2010.

Published online September 16, 2010.  
10.1021/nn100465s

© 2010 American Chemical Society

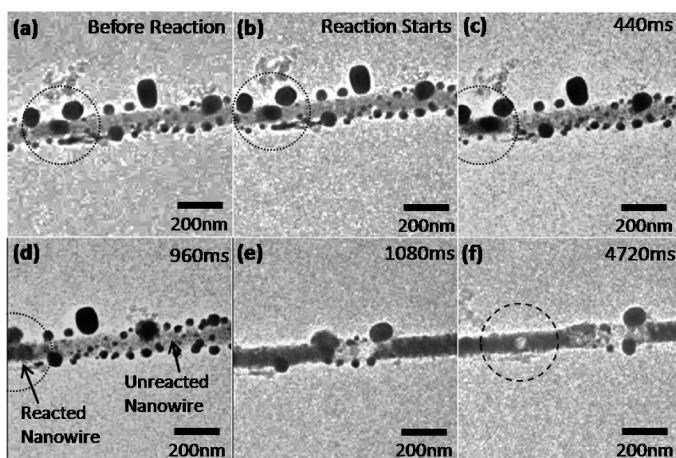


**Figure 1.** (a) The Ni coating formed droplets on the native oxide before the transformation. (b–d) Formation process of NiSi<sub>2</sub>. (e,f) The starting point of the reaction is indicated by the circles. (e) The nanowire is completely transformed into NiSi<sub>2</sub>. (f) The NiSi<sub>2</sub> nanowire starts to evaporate by further increasing the temperature. The numbers at upper right are the video recording time.

instantly. The resulting nanowires were single crystalline NiSi<sub>2</sub> for those Si nanowires containing thick native oxide shells. Si nanowires with (or without) thin oxide layers always formed polycrystalline Ni silicides of different phases.

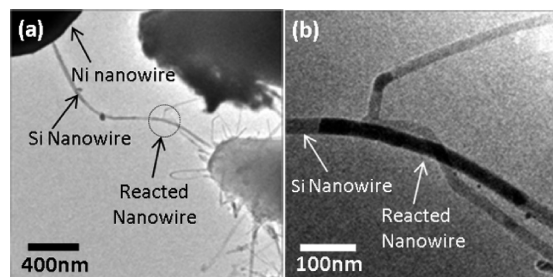
## RESULTS AND DISCUSSION

Figure 1 panels a–f demonstrate the *in situ* observation of the structural change process of the Ni-coated silicon nanowire as recorded by a video camera. Because of the native oxide, the Ni layer could not react directly with the Si nanowire at temperatures below 1350 °C (the heating filament temperature). Instead, Ni atoms segregated and formed different sizes of nanodroplets (Figure 1a) at about 1300 °C.<sup>16</sup> Some Ni droplets migrated together resulting in large droplets (50–100 nm in diameter). When the temperature was slightly above 1350 °C, most Ni droplets were suddenly “dissolved” into the Si nanowire. This reaction was surprisingly fast and finished instantly. The temperature mentioned above is the surface temperature of the heating filament we calibrated (see also the description in Experimental Details). Such a high temperature is needed to start the phase transformation of Si nanowires (with thick oxide shells) with Ni. After phase

transformation, the resulted Ni–silicide nanowires formed a NiSi<sub>2</sub> structure as observed by the selected-area electron diffraction (SAED) patterns at room temperature. According to the frames recorded by the video camera (Figure 1d,e), the time needed for this phase transformation is less than 0.1 s. We noted that the reaction or structure transformation initially started at one location of the nanowire as marked by the circle in Figure 1 panels c and d. Then, the NiSi<sub>2</sub> grain grew along the nanowire rapidly from this special location. We have not observed multisite nucleation of NiSi<sub>2</sub> in the Si nanowires with thick cladding native oxide. It is apparent that at an elevated temperature, the nucleation site for the phase transformation should be a defect site at which the diffusion of Ni can easily take place. The resulted NiSi<sub>2</sub> nanowires as shown in Figure 1e and Figure 4b,c displayed uniform contrast because they were single crystalline as identified by SAED. The SAED patterns taken from these silicide nanowires can be indexed by the NiSi<sub>2</sub> structure. Figure 4c is an example of these patterns which are obtained by tilting the heating stage within a limited tilting angle.

Using the STM manipulator, we can move Si nanowires to touch the heating filament. Then, further movement toward the filament can cause bending of the nanowires. As shown in Figure 2a, we placed Ni on the filament in order to generate Ni vapor source. We observed that the nucleation of NiSi<sub>2</sub> crystals always occurred preferentially at the heavily bending regions of the nanowire (see Figure 2b). Such bending may result in defects such as cracks on the oxide clad. Therefore, these defects provide the channels for Ni fast diffusion and the preferential nucleation sites for Ni silicides. In Figure 2a, the Si nanowire tip which contacted the Ni wire should gain a higher temperature. But, the reaction did not happen on this high temperature region. The bending regions are always the preferential reaction places for Ni.

The formation of single crystalline NiSi<sub>2</sub> nanowires in the present condition benefits from the thick clad native oxide on the Si nanowires. This is because the native oxide protects the Si cores from reaction with Ni at relatively low temperatures. For Si nanowires with no clad oxide, the Ni coating layer can directly react with Si to preferentially form some other Ni silicide structures at certain temperatures. For example, a NiSi structure can easily form at about 550 °C.<sup>15</sup> According to our experience, because of the presence of the oxide layers, the actual reaction temperature for Si nanowires is over 1350 °C (the filament temperature) which is higher than the temperature (850 °C) normally required for the formation of NiSi<sub>2</sub>. To confirm our explanation for the formation of NiSi<sub>2</sub>, we have removed the clad oxide from the Si nanowire surfaces using chemical etching (2% HF acid) treatment and repeated the *in situ* experiment. The



**Figure 2.** (a) The point contact annealing for Ni and bending Si nanowires. The circle indicates the reacted regions. (b) Enlarged picture of the nanowires marked by the circle.

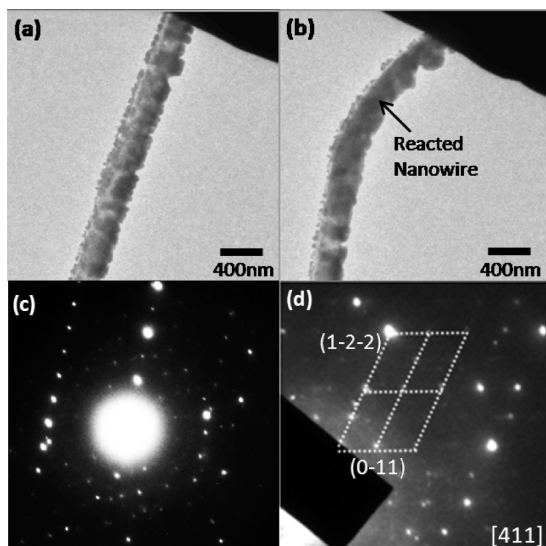


**Figure 3.** (a) The Si nanowire treated by HF and then coated with Ni before the transformation. (b) The reaction started without forming Ni droplets. Panels c and d are the SAED pattern of the resulted silicide nanowire shown in panel b. The nanowire is polycrystalline. Some of the diffraction spots can be indexed by the diffractions of  $\text{Ni}_{31}\text{Si}_{12}$  along the zone axis of [411].

phase transformation occurred at about 650 °C. At this temperature, the Ni layer was still in the solid state. As shown in Figure 3a,b, the reaction started at the high temperature region (close to the heating filament) and gradually extended to the entire nanowire. The resulting Ni silicide nanowire was polycrystalline and contained more than one phase as identified by the selected-area electron diffraction shown in Figure 3c. One of the silicide structures has been determined to be  $\text{Ni}_{31}\text{Si}_{12}$  (see Figure 3d). From our investigation, the native oxide shells acted as the reaction barriers to effectively resist the formation of different phases of Ni silicides. This finding also indicated a method for fabricating high quality  $\text{NiSi}_2$  nanowires or  $\text{NiSi}_2/\text{Si}$  nanowire junctions. Since the reaction temperature for the Si nanowires with thick oxide shells is high, the growth rate of  $\text{NiSi}_2$  is much faster than that of the Ni silicide fabricated by the point-contact reaction (0.11 nm/s) as reported by Lu *et al.*<sup>5</sup>

In previous studies,<sup>17,18</sup> several methods for converting Si nanowires to  $\text{NiSi}_2$  nanowires have been reported. Using arc ion implantation in vacuum, we have synthesized  $\text{NiSi}_2/\text{Si}$  structure on Si nanowire surfaces. The high-energy Ni ions (5 kV) were implanted into Si to form a mixture of Ni/Si clusters on one side of the nanowire. The subsequent rapid annealing resulted in polycrystalline  $\text{NiSi}_2$  structure. However, it was difficult to improve the quality of these silicide nanowires by further annealing at a higher temperature because a too high annealing temperature caused change of the nanowire morphology. Zeng *et al.*<sup>17</sup> reported a sputtering method to coat Si nanowires using the Ni ions with a relative low kinetic energy (about 18 eV).<sup>19</sup> They sug-

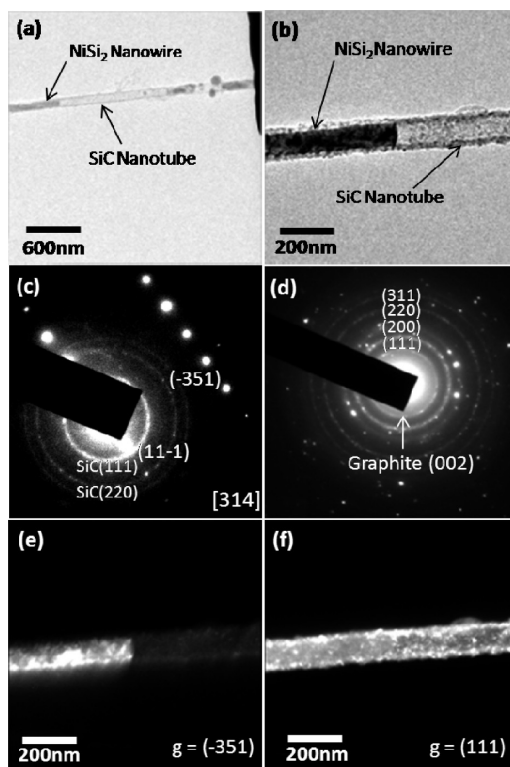


**Figure 4.** (a, b) The morphology of the heterojunction of the  $\text{NiSi}_2$  nanowire and SiC nanotube. (c) The SAED of the  $\text{NiSi}_2$  nanowire viewed along the [314] zone axis. (d) The SAED of the SiC nanotube. The diffraction rings have been indexed by the cubic SiC plus the (002) diffraction of graphite. (e, f) The dark field images of the  $\text{NiSi}_2/\text{SiC}$  heterojunction shown in panel b. The  $\text{NiSi}_2$  nanowire appeared bright in panel e when using the  $(-351)$  diffraction (shown in panel c) for imaging, while the SiC nanotube was bright when using the diffraction ring (111) in panel d for imaging.

gested that because of the damaging or implantation effect some Ni ions could be implanted into the nanowire surface region. Consequently, the nucleation of the Ni silicides started at everywhere throughout the nanowire simultaneously, resulting in polycrystalline  $\text{NiSi}_2$ . According to our *in situ* observation, the Ni atoms diffused into the nanowire core through some special regions of the native oxide shells. However, the shells were unchanged after the formation of  $\text{NiSi}_2$ . By further increasing the filament temperature, the  $\text{NiSi}_2$  nanowire could be evaporated gradually leaving an empty shell or a nanotube structure (see Figure 4a,b). It is interesting to note that the native oxide shells have been converted to polycrystalline  $\beta\text{-SiC}$  during the phase transformation of  $\text{NiSi}_2$ . Figure 4 panels e and f illustrate the dark-field images of the core-shell nanostructure, that is, the  $\text{NiSi}_2$  core is wrapped by a SiC shell (about 15 nm thick). The  $\text{NiSi}_2$  nanowire appeared bright in Figure 4e when using the  $(-351)$  diffraction for imaging, while the SiC nanotube showed no contrast. However, when using the diffraction ring (111) of the  $\beta\text{-SiC}$  in Figure 4d for imaging, the nanotube appeared bright. As identified by the SAED patterns in Fig-

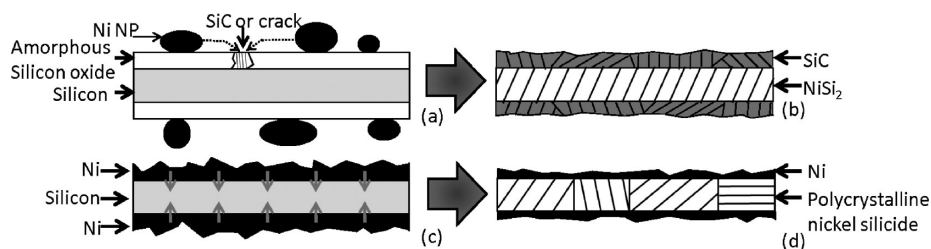


**Figure 5.** The formation mechanisms of the Ni silicides nanowires and SiC heterojunction. (a) The catalytic effect of Ni may result in the formation of SiC in the native oxide shells and this causes cracks or other defects. Ni atoms can diffuse into the Si nanowire through these defects. (b) After Ni atoms penetrate the native oxide to react with the Si core, the released carbon will react with the oxide shell to form SiC. (c–d) The reaction mechanism for the Si nanowire without clad oxide. Ni atoms can directly react with the Si wire at low temperatures everywhere and thus result in polycrystalline silicide nanowire by the multisite nucleation.

ure 4c,d, the NiSi<sub>2</sub> wire was single crystalline and the SiC nanotube was polycrystalline.

For the formation of SiC nanotube structure, the carbon source should come from the hydrocarbon molecules of the diffusion pump oil in the TEM chamber. It is well-known that the hydrocarbon contamination has to be reduced by a liquid nitrogen cold trap in TEM. In this *in situ* study, the liquid nitrogen trap was not used due to the heating experiment. We believed that the Ni coating decomposed the hydrocarbon molecules during the heating process. This is because Ni is an excellent catalyst and has been extensively used for catalytic growth of carbon nanotubes and graphene sheets.<sup>20–26</sup> The weak diffraction ring of (002) from graphite structure can be seen in the SAED pattern in Figure 4d. When the Ni atoms “dissolve” into the Si core, the carbon in the Ni droplets has to be drained out, as there is no stable Ni–Si–C compound at 1300–1400 °C.<sup>27</sup> With the assistance of the Ni catalytic effect, the Si oxide shells can react with carbon to form SiC shells at 1300–1400 °C<sup>28</sup> through the following reaction:



Figure 5 panels a and b schematically illustrate these reaction mechanisms. We believe that the speed of reaction 1 was slow at about 1300 °C (the filament temperature). At some regions of the native oxide shell, the formation of SiC grains may generate cracks (Figure 5a) on the shell and thus open up channels for Ni diffusion and reaction with the Si core. Since the reaction temperature is sufficiently high, the NiSi<sub>2</sub> nanowire is single crystalline. For the Si nanowire without native oxide clad (Figure 5c), phase transformation can start everywhere at a relative low temperature, resulting in

polycrystalline Ni silicide grains (Figure 5d). The Ni–Si<sub>2</sub>/Si and NiSi<sub>2</sub>/SiC nanoheterostructures are promising for potential technological applications in electrical nanodevices. For example, the junctions of Ni silicide on SiC have been determined to be an excellent non-uniform Schottky barrier with a low contact resistance ( $3.6 \times 10^{-5} \Omega\text{cm}^2$ ), an ideality factor  $n = 1.07$  (a measure of how closely the diode follows the ideal diode equation) and a good barrier height of about 1.3 eV.<sup>29</sup> Since the quality of the SiC shells is not good enough for devices, further experiments are needed to improve or eliminate the formation of SiC by using a controlled carbon source and a dry pump such as a turbomolecular-pump instead of an oil diffusion pump in order to control and improve the quality of the SiC shells formed on the Ni-silicide nanowires. Further study on the characterization of the electrical transport properties of the NiSi<sub>2</sub>/Si and NiSi<sub>2</sub>/SiC nanoheterostructures is in progress.

In summary, we have observed interesting structural transformation behaviors and reaction processes from Ni-coated Si nanowires using a specially designed heating filament integrated with a commercial scanning tunneling microscopy manipulator. The reaction between Ni and Si nanowires started preferentially at bending regions. The native oxide on the Si nanowires played a critical role for the formation of single crystalline NiSi<sub>2</sub>. The structural transformation in the Si nanowires containing thick native oxide usually happened at a relatively high temperature, and the resulted Ni silicide nanowires were single crystalline NiSi<sub>2</sub>. Nanowire junctions of NiSi<sub>2</sub>/Si and nanowire–nanotube junctions of NiSi<sub>2</sub>/SiC have been obtained upon further annealing.

## EXPERIMENTAL DETAILS

Si nanowires were fabricated on a Si wafer with gold nanoparticles as the catalysts. The Si vapor source was silane gas (purity > 99.99 and flow rate 15 sccm) which was mixed with hydrogen (purity > 99.99% and flow rate of 100 sccm) and fed into the reaction quartz tube (pressure was about 50 Torr) placed in a furnace. High-quality Si nanowires grew at about 520 °C. The *in situ* experiments were carried out in a high-resolution transmis-

sion electron microscope (HRTEM, JEOL-2011) operated at 200 kV. The heating stage is homemade and integrated with a commercial scanning tunneling microscopy (STM) manipulator (Nanofactory Instrument) working under a high vacuum condition ( $10^{-5}$  Pa). Figure 6a shows the schematic diagram of this experimental setup. Different from the commercial *in situ* TEM technique,<sup>9–12</sup> this STM-integrated heating stage is more suitable for nanowires manipulation, reaction, and structure investi-

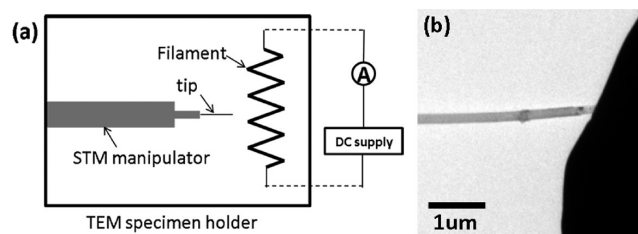


Figure 6. (a) The schematic diagram of the experimental setup. (b) The silicon nanowire coated with nickel is approaching the heating filament.

gation. In recent years, the *in situ* HRTEM technique has become a powerful tool for investigating the reaction of nanosized material at the atomic level.<sup>13,14</sup>

To realize the *in situ* observation of the nanowire reaction and structural transformation, Si nanowires precoated with Ni (about 50 nm thick) were mounted on the STM manipulator tip which was integrated into the TEM specimen holder. The heating element was a tungsten filament, and its temperature was controlled by a DC current source. Under TEM observation, the Si nanowires were delicately driven by the STM tip to approach the heating filament. Once the contact between the Si nanowire and the filament was established (see Figure 6b), a DC current was supplied to the filament to locally heat the nanowire sample. We used different materials to calibrate the relationship between the filament surface temperature and the DC current applied to the filament. Because of this special heating method, the actual temperature on the nanosized samples may deviate from that calibrated for the filament. As tested for the sublimation temperature of a ZnO rod and the melting temperature of a thick Si wire, the temperatures measured was about 500 and 1400 °C respectively, which are quite close to the sublimation temperature of ZnO (~500 °C)<sup>15</sup> and the melting point of Si crystals (1414 °C). Using the calibrated temperature–filament current relation, we measured the transformation temperature of the Ni–silicide nanowires.

**Acknowledgment.** The authors are grateful for financial support from the Research Grants Council of Hong Kong (Project Nos. CityU5/CRF/08, 603408, 604009).

## REFERENCES AND NOTES

- Wu, Y.; Xiang, J.; Yang, C.; Lu, W.; Lieber, C. M. Single-Crystal Metallic Nanowires and Metal/Semiconductor Nanowire Heterostructures. *Nature* **2004**, *430*, 61–65.
- Sun, Z. Q.; Whang, S. J.; Yang, W. F.; Lee, S. J. Synthesis of Nickel Mono-silicide Nanowire by Chemical Vapor Deposition on Nickel Film: Role of Surface Nickel Oxides. *Jpn. J. Appl. Phys.* **2009**, *48*, 04C138.
- Kim, J.; Anderson, W. A. Spontaneous Nickel Monosilicide Nanowire Formation by Metal Induced Growth. *Thin Solid Films*. **2005**, *483*, 60–65.
- Decker, C. A.; Solanki, R.; Freeouf, J. L.; Carruthers, J. R.; Evans, D. R. Directed Growth of Nickel Silicide Nanowires. *Appl. Phys. Lett.* **2004**, *84*, 1389–1391.
- Lu, K. C.; Tu, K. N.; Wu, W. W.; Chen, L. J.; Yoo, B. Y.; Myung, N. V. Point Contact Reactions Between Ni and Si Nanowires and Reactive Epitaxial Growth of Axial Nano-NiSi/Si. *Appl. Phys. Lett.* **2007**, *90*, 253111–253111-3.
- Lu, K. C.; Wu, W. W.; Wu, H. W.; Tanner, C. M.; Chang, J. P.; Chen, L. J.; Tu, K. N. *In Situ* Control of Atomic-Scale Si Layer with Huge Strain in the Nanoheterostructure NiSi/Si/NiSi through Point Contact Reaction. *Nano Lett.* **2007**, *7*, 2389–2394.
- Zhang, Z.; Hellstrom, P. E.; Ostling, M.; Zhang, S. L.; Lu, J. Electrically Robust Ultralong Nanowires of NiSi, Ni<sub>2</sub>Si, and Ni<sub>3</sub>Si<sub>2</sub>. *Appl. Phys. Lett.* **2006**, *88*, 043104–043104-3.
- Liu, W. L.; Chen, W. J.; Tsai, T. K.; Tsai, H. H.; Hsieh, S. H. Interface Structure Between Epitaxial NiSi<sub>2</sub> and Si. *J. Univ. Sci. Technol. Beijing*. **2006**, *13*, 558–563.
- Wall, M. A.; Dahmen, U. *An In Situ* Nanoindentation Specimen Holder for a High Voltage Transmission Electron Microscope. *Microsc. Res. Tech.* **1998**, *42*, 248–254.
- Kizuka, T.; Tanaka, N.; Deguchi, S.; Naruse, M. Time-Resolved High-Resolution Transmission Electron Microscopy Using a Piezo-Driving Specimen Holder for Atomic-Scale Mechanical Interaction. *Microsc. Microanal.* **1998**, *4*, 218–225.
- Wang, M. S.; Golberg, D.; Bando, Y. Interface Dynamic Behavior between a Carbon Nanotube and Metal Electrode. *Adv. Mater.* **2009**, *22*, 93–98.
- Liao, C. N.; Chen, K. C.; Wu, W. W.; Chen, L. J. *In Situ* Transmission Electron Microscope Observations of Electromigration in Copper Lines at Room Temperature. *Appl. Phys. Lett.* **2005**, *87*, 141903–141903-3.
- Liu, C. H.; Wu, W. W.; Chen, L. J. Collective Movement of Three Million Plus Au Atoms on a Silicon Bicrystal. *Appl. Phys. Lett.* **2006**, *88*, 023117–023117-2.
- Helveg, S.; Lopez-Cartes, C.; Sehested, J.; Hansen, P. L.; Clausen, B. S.; Rostrup-Nielsen, J. R.; Abild-Pedersen, F.; Nørskov, J. K. Atomic-Scale Imaging of Carbon Nanofiber Growth. *Nature* **2004**, *427*, 426–429.
- Wurster, D. E.; Oh, E.; Wang, J. C. T. Determination of The Mechanism for the Decrease in Zinc Oxide Surface Area Upon High-Temperature Drying. *J. Pharm. Sci.* **1995**, *84*, 1301–1307.
- Jiang, Q.; Tong, H. Y.; Hsu, D. T.; Okuyama, K.; Shi, F. G. Thermal Stability of Crystalline Thin Films. *Thin Solid Films* **1998**, *312*, 357–361.
- Jiang, S.; Xin, Q.; Chen, Y.; Lou, H.; Lv, Y.; Zeng, W. Preparation of NiSi<sub>2</sub> Nanowires with Low Resistivity by Reaction between Ni Coating and Silicon Nanowires. *Appl. Phys. Express* **2009**, *2*, 075005–075005-3.
- Lee, C. Y.; Lu, M. P.; Liao, K. F.; Lee, W. F.; Huang, C. T.; Chen, S. Y.; Chen, L. J. Free-Standing Single-Crystal NiSi<sub>2</sub> Nanowires with Excellent Electrical Transport and Field Emission Properties. *J. Phys. Chem. C* **2009**, *113*, 2286–2289.
- Tian, M. B. *Thin Film Technologies and Materials*; Tsinghua University Press: Beijing, 2006; pp 464.
- Yudasaka, M.; Kikuchi, R.; Matsui, T.; Ohki, Y.; Yoshimura, S. Specific Conditions for Ni Catalyzed Carbon Nanotube Growth by Chemical Vapor Deposition. *Appl. Phys. Lett.* **1995**, *67*, 2477–2479.
- Reina, A.; Jia, X.; Ho, J.; Nezhich, D.; Son, H.; Bulovic, V.; Dresselhaus, M. S.; Kong, J. Large Area, Few-Layer Graphene Films on Arbitrary Substrates by Chemical Vapor Deposition. *Nano Lett.* **2009**, *9*, 30–35.
- Li, X.; Cai, W.; Colombo, L.; Ruoff, R. S. Evolution of Graphene Growth on Ni and Cu by Carbon Isotope Labeling. *Nano Lett.* **2009**, *9*, 4268–4272.
- Thiele, S.; Reina, A.; Healey, P.; Kedzierski, J.; Wyatt, P.; Hsu, P.; Keast, C.; Schaefer, J.; Kong, J. Engineering Polycrystalline Ni Films to Improve Thickness Uniformity of the Chemical–Vapor–Deposition-Grown Graphene Films. *Nanotechnology* **2010**, *21*, 015601–015601-8.
- Chae, S. J.; Gunes, F.; Kim, K. K.; Kim, E. S.; Han, G. H.; Kim, S. M.; Shin, H. J.; Yoon, S. M.; Choi, J. Y.; Park, M. H.; et al. Synthesis of Large-Area Graphene Layers on Polynickel Substrate by Chemical Vapor Deposition: Wrinkle Formation. *Adv. Mater.* **2009**, *21*, 2328–2333.

25. Jung, M.; Eun, K. Y.; Lee, J.; Baik, Y. J.; Lee, K.; Park, J. W. Growth of Carbon Nanotubes by Chemical Vapor Deposition. *Diamond Relat. Mater.* **2001**, *10*, 1235–1240.
26. Ho, G. W.; Wee, A. T. S.; Lin, J.; Tjiu, W. C. Synthesis of Well-Aligned Multiwalled Carbon Nanotubes on Ni Catalyst Using Radio Frequency Plasma-Enhanced Chemical Vapor Deposition. *Thin Solid Films.* **2001**, *388*, 73–77.
27. Kuznetsov, V.; Usoltseva, A.; Mazov, I. Carbon Nanotubes' and Silicon Carbide Whiskers' Growth on Metal Catalysts: Common Features of Formation Mechanisms. *Mater. Res. Soc. Symp. Proc.* **2005**, *858E*, HH3.14.1HH3.14.6.
28. Miller, P. D.; Lee, J. G.; Cutler, I. B. The Reduction of Silica with Carbon and Silicon Carbide. *J. Am. Ceram. Soc.* **1979**, *62*, 147–149.
29. Via, F. L.; Roccaforte, F.; Makhtari, A.; Raineri, V.; Musumeci, P.; Calcagno, L. Structural and Electrical Characterisation of Titanium and Nickel Silicide Contacts on Silicon Carbide. *Microelectron. Eng.* **2002**, *60*, 269–282.